COMPUTATIONAL ANALYSIS STUDY OF AERODYNAMIC VEHICLE PASSENGER CAR (FRONT GRILL)

MUHAMAD KHAIRUL HAKIMI BIN HAMID

Thesis submitted in fulfillment of the requirements
for the awards of the degree of Bachelor of Mechanical Engineering

Faculty of Mechanical Engineering
UNIVERSITI MALAYSIA PAHANG

JUNE 2012

ABSTRACT

Designing the front grill with the focus on an improvement aspect is very important in the automotive industry. This study proposes are to increase performance of the front grille and study effect of aerodynamic flow through the front grill using Computational Fluid Dynamic CFD. The difference speed which is at 80km/h, 120km/h and 180km/h was applied to obtain the flow structure around a passenger car with three design consideration of front grill. In this paper, the CFD simulation of Ansys FLUENT flow was applied to measure the result in the wind tunnel of passenger car design. The numerical method required to solve the Nervier–Stokes equations for incompressible and three-dimensional fluid motion. Result from three different discretization are compared with the past experiment data. In general, the characteristic of velocity and pressure counters was compared with three different speeds by symmetrical plane. Validation of drag and pressure effected on front grill also discussed to optimize the best aerodynamic flow of passenger car to all three design. Finally, the aerodynamics of the best design of front grill are introduced and analyzed.

ABSTRAK

Merekabentuk gril hadapan dengan tumpuan pada aspek peningkatan adalah sangat penting dalam industri automotif. Kajian ini mencadangkan untuk meningkatkan prestasi gril depan dan kesan kajian aliran aerodinamik melalui gril hadapan dengan menggunakan Komputasi Bendalir Dinamik CFD. Perbezaan kelajuan yang di 80km / j, 120km/j dan 180km/j telah digunakan untuk mendapatkan struktur aliran di sekitar kereta penumpang dengan tiga reka bentuk pertimbangan gril hadapan. Dalam kertas ini, simulasi CFD aliran Anys FLUENT telah digunakan untuk mengukur hasil dalam terowong angin pada reka bentuk kereta penumpang. Kaedah berangka yang diperlukan untuk menyelesaikan persamaan Nervier-Stokes untuk tidak boleh mampat dan tiga dimensi gerakan bendalir. Keputusan daripada tiga pendiskretan yang berbeza dibandingkan dengan data eksperimen yang lalu. Secara umum, ciri-ciri halaju dan kaunter tekanan dibanding dengan tiga kelajuan yang berbeza pada paksi simetri. Pengesahan heretan dan tekanan yang dilaksanakan pada gril hadapan juga dibincangkan untuk mengoptimumkan aliran aerodinamik kereta penumpang bagi ketiga-tiga reka bentuk tersebut. Akhir sekali, aerodinamik reka bentuk yang terbaik gril hadapan diperkenalkan dan dianalisis.

TABLE OF CONTENTS

		Page
SUPERVISOR'S DECLARATION		ii
STUDENT'S DECLARATION		iii
ACKNOWLEDGEMENTS		iv
ABSTRACT		v
ABSTRAK		vi
TABLE OF CONTENTS		vii
LIST OF TABLES		x
LIST OF FIGURES		xi
LIST OF SYMBOLS		xiii
LIST OF ABBREVIATIONS		xiv
CHAPTER 1	**INTRODUCTION**	
1.1	Background	1
1.2	Problem Statement	2
1.3	Project Objectives	2
1.4	Project Scopes	2
CHAPTER 2	**LITERATURE REVIEW**	
2.1	Computational Fluid Dynamics	3
	2.1.1 General CFD	3
	2.1.2 Navier-Stroke Equation	4
	2.1.3 Reynolds Average Navier Stroke (RANS)	4
2.2	Turbulence Model	5
	2.2.1 K-e Turbulence model	6
	2.2.2 Boundary Layers And Wall Function	7
2.3	Aerodynamic	8
	2.3.1 Aerodynamic Force	9
	2.3.1.1 Drag Force and Drag Coefficient	10

2.3.1.2 Lift Force and Lift Coefficient 10
2.3.1.3 Pressure Coefficient 10

2.4 Front Grill 11

2.4.1 Airflow Ducting Between Air Intake and Radiator 11
2.4.2 Location and Size of Front End Openings 12

2.5 Previous Work 13

CHAPTER 3 METHODOLOGY

3.0 Introduction 15

3.1 Flow Chart of Project 16

3.1.1 Project Introduction 17
3.1.2 Literature Study 17
3.1.3 Problem Solving 17

3.2 Computational Fluid Dynamic (CFD) Analysis Simulation 18

3.2.1 Generic Model 18
3.2.2 Front Grill Design 19
3.2.3 Mesh Generation 20
3.2.4 Simulation Model 20
3.2.5 Method of Attack 21
3.2.6 Solver Setting 21

CHAPTER 4 RESULT AND DISCUSSION

4.1 Introduction 23

4.2 Velocity Contours 24

4.3 Pressure Contours 25

4.4 Overhanging Curve 27

4.5 Velocity Vector 27

4.6 Drag Coefficient 30

4.7 Pressure coefficient 32

4.8 The Best Design 34

4.9 Comparisson of Pressure Coefficient 35

CHAPTER 5 CONCLUSION AND RECOMMENDATION

5.1	Conclusion	37
5.2	Recommendation	38

REFERENCES 39

APPENDICES 41

A Gantt Chart For Final Year Project 1 41

B Gantt Chart For Final Year Project 2 42

LIST OF TABLES

Table No.	Title	Page
1.0	Solver and boundary condition setting.	22

LIST OF FIGURES

Fig. No	Title	Page
2.1	Velocity profile in the near wall region for a turbulence boundary layer	7
2.2	Comparison of low and high aerodynamic drag forces with rolling Resistance	8
2.3	Flow around a passenger car (external flow).	9
2.4	Influence of ducting between air intake and radiator on radiator flow velocity.	11
2.5	Influence of air intake location and size on aerodynamic performance (measured on a full scale test vehicle)	12
2.6	Flow separations at front and rear part of Ahmed model geometry	13
3.1	Generic model of front grill and passenger car.	18
3.2	Design of front grill	19
3.3	Meshing characteristics were used in the wind tunnel.	20
3.4	Wind tunnel layout and the model car inside the tunnel	21
4.1	Velocity contour at velocity 80 km/h	24
4.2	Velocity contour at velocity 120 km/h	25
4.3	Velocity contour at velocity 180 km/h	25
4.4	Pressure contour at velocity 80 km/h	26
4.5	Pressure contour at velocity 120 km/h	26
4.6	Pressure contour at velocity 180 km/h	26
4.7	Counters of static pressure of the overhanging curve.	27
4.8	Velocity vectors at 80 km/h of the airflow over the front grill	29
4.9	Velocity vectors at 50 m/s of the air flow over the front grill	30
4.10	Drag coefficient at velocity 16.67 m/s	31

4.11	Drag coefficient at velocity 33.33 m/s	31
4.12	Drag coefficient at Velocity 50 m/s.	32
4.13	Pressure Coefficient, Cp of flow upperbody and underbody.	33
4.14	Vaious configuration of front grill design	34
4.15	Comparisons of lift and drag coefficient for the three design at maximum speed 180km/h	35
4.16	Comparisson of pressure coefficient for all design with the Tsai et al experiment	36

LIST OF SYMBOLS

ρ	Vescosity
p	Pressure
W	Work
v	Velocity
m	Meter
s	Second
t	Time
h	Hour
%	Percent
Cd	Drag coefficient.
Cl	Lift coefficient
A	Frontal area
Pa	Pascal
L	Length
w	Width
H	High

LIST OF ABBREVIATIONS

k-e	K-epsilon
k-ω	K-omega
W	Weight
CFD	Computer Fluid Dynamic
T	Time
R	Radius Of Cornering
RANS	Reynold Averaged Navier Stroke
RNG	Re-Normalisation Group
SAE	Society of Automotive Engineer
LES	Large Eddy Simulation
CW	Clockwise
CCW	Counter clockwise

CHAPTER 1

INTRODUCTION

1.1. Background

Nowadays, road vehicle tends to develop lift thrust of the body. Base of the passenger car design, the upper aerodynamic shape will provide smooth to let airflow moving faster through the body. During high speed, pressure distribution at upper and underneath vehicle is different. The lift force occurs when air pressure at underneath is greater than upper air pressure. It does depend on the velocity of airflow surround the vehicle. According to Bernoulli principle, when velocity increase the pressure will decrease and otherwise.

This project will focus on study aerodynamic flow for passenger car with the air flow through the front end of a vehicle. Car manufacturers are taking this into consideration when designing a vehicle. Since many contradicting factors are defining the front end design, a clear understanding of the airflow behavior and drag influence on the passenger car is required. Many have resorted to computational fluid dynamic (CFD) to get this understanding.

When investigating the aerodynamics behavior of a vehicle, wind tunnel test is often a good tool but has a high cost and often takes place late in the development process which makes it hard to make any modifications. An alternative or complement to running full-scale wind tunnel test is using simulation tools as CFD codes which enable the possibility to make modifications early in the development process.

To obtain better performance of air flow and aerodynamic performance by the shape of the front grill and the discharge flow field Underhood and body impact the area

requirement. The greater airflow need drives larger frontal opening with less restrictive grill texture. Pressure drop should be kept as low as possible and the frontal grill opening will increase vehicle drag and reduce fuel economy (W.Kieffer et al 2005). At first the objective was to study the air flow through the front grill with increase the negative lift force (down force) by accelerating the underbody airflow.

1.2. Problem Statement

From the previous research or analysis on the front end of the aerodynamic vehicle like as a passenger car, basically focus on the general external flow suppression on the vehicle body and wake region. However, for this analysis, it is mainly focused on the study flow through the front grill using three different design models of front grill by applying different flow velocity. From the flow, it will influence the lift, drag and underbody affected on the of passenger car.

1.3. Project Objectives

Basically the main purpose in accomplishing this task is stated below

i. To study the flow through of front grill using the Computational Fluid Dynamic-CFD .
ii. To study the effect of aerodynamic flow in the front grill.
iii. Towards a better understanding of the interaction of front grill and aerodynamic performance.

1.4. Scopes of Project

The scope of this project is focusing on the criteria that stated below

i. Analysis flow from passenger car using 3 difference models of the front grill.
ii. Analysis flow speed through the wind tunnel.
iii. Variable flow speed at 80 km/h, 120 km/h and 180 km/h at steady state condition.
iv. Three design consideration.

CHAPTER 2

LITERATURE REVIEW

2.1. Computational fluid dynamics (CFD)

CFD is a numerical method to compute and analyze the dynamics of a fluid. The approach for a CFD simulation is to divide the physical domain into small finite volume elements where the governing equations are solve numerical. Almost all flows are turbulent, to spare computer capacity so called turbulence model can be used to simulate the turbulence. In the following sections the governing equations are presented as well as turbulence model.

2.1.1. General CFD

In fluid dynamic there are three equations describe the behavior of the flow, these are continuity, momentum and energy equations. They are derives from basic physics laws as the conservation of energy, mass and momentum. These equations become rather complicated and cannot be solved analytic, so numerical simulation are required.

In a CFD simulation the differential equations are discritize into large system of algebraic equations in order to numerical solve them. Since vehicle travels at relatively low speed, Ma<0.3, and constant temperature the flow can be assumed incompressible and isothermal, the energy equation can be neglected (Jesper Marklund).

2.1.2. Navier-Stroke Equation

Navier-Stroke equations are derived from Newtons second law and can be seen as a force equilibrium for an infinitesimal small volume element. In order to convert the stress to velocity components the Navier-stroke equation are usually expressed for an incompressible Newton fluid with constant viscosity. An incompressible fluid is a fluid where the divergence of the velocity is zero, and a Newtonian fluid is a fluid which stress versus strain rate curve is linear. The Navier-Strokes equations can be expressed as in Eq.(1-3), three partial non-linear differential equation, one for each velocity vector (Frank M. White 2008).

$$\rho g_x - \frac{\partial y}{\partial x} + \mu\left(\frac{\partial^2 u}{\partial x^2} + \frac{\partial^2 u}{\partial y^2} + \frac{\partial^2 u}{\partial x^2}\right) = \rho\frac{du}{dt} \tag{1}$$

$$\rho g_x - \frac{\partial p}{\partial y} + \mu\left(\frac{\partial^2 v}{\partial x^2} + \frac{\partial^2 v}{\partial y^2} + \frac{\partial^2 v}{\partial x^2}\right) = \rho\frac{dv}{dt} \tag{2}$$

$$\rho g_z - \frac{\partial p}{\partial z} + \mu\left(\frac{\partial^2 w}{\partial w^2} + \frac{\partial^2 w}{\partial y^2} + \frac{\partial^2 w}{\partial x^2}\right) = \rho\frac{dw}{dt} \tag{3}$$

Continuity equation is based on the principle that the mass is indestructible, and can be written as Eq (4).

$$\frac{\partial \rho}{\partial t} + \frac{\partial(\rho u)}{\partial x} + \frac{\partial(\rho u)}{\partial y} + \frac{\partial(w)}{\partial z} = 0 \tag{4}$$

Since the flow is assumed incompressible the continuity equation will be as in Eq. (5).

$$\frac{\partial u}{\partial x} + \frac{\partial v}{\partial y} + \frac{\partial w}{\partial z} = 0 \tag{5}$$

2.1.3. Reynolds Average Navier Stroke (RANS)

The non-linear partial differential equations are not analytically. In order to solve these equation and analyze the flow the simplest is the Reynolds decomposition, also

called Reynolds Average Navier Stroke (RANS). (W. Malalasekera). In the RANS approach the Instantaneous velocity and pressure is split into two part, an average part and a fluctuating part, Eq. (4) and Eq.(5).

$$u = \frac{1}{T}\int_0^T u\, dt \tag{6}$$

$$p = \bar{p} + \acute{p} \tag{7}$$

Inserting Reynolds decomposition into Navier-Stokes equation (x-direction) and in the continuity equation will result in new fluctuating terms.

$$\frac{\partial \bar{u}}{\partial x} + \frac{\partial \bar{v}}{\partial y} + \frac{\partial \bar{w}}{\partial z} = 0 \tag{8}$$

$$\rho g_x - \frac{\partial \bar{p}}{\partial x} + \frac{\partial}{\partial x}\left(\mu \frac{\partial \bar{u}}{\partial x} - \rho\overline{u^{r2}}\right) + \frac{\partial}{\partial y}\left(\mu \frac{\partial}{\partial y} - \rho\overline{u^2 v^2}\right) + \frac{\partial}{\partial z}\left(\mu \frac{\partial \bar{u}}{\partial z} - \rho\overline{u^2 w^2}\right) = \rho \frac{d\bar{u}}{dt} \tag{9}$$

Eq. (7) now consists of new unknown terms like $\boldsymbol{\rho\overline{u^2 w^2}}$, also called for Reynolds stress, sure the number of unknown are greater then the number of equation a so called closure problem is generated, the extra stress terms has to be modeled to get a closed a equation system. This is done by using turbulence models (Frank M. White).

2.2. Turbulence Model

Turbulence models the flow field can be calculated with less computer capacity. Such a model will modify the equations and only consider the average effects of the turbulence. The flow will then be divided into an average term and fluctuation term, this can be done using Reynolds Average Navier Strokes (RANS). A turbulence model can never give an exact solution, but a better choice will give an more accurate solution. The choice of models is a matter of computer capacity and required level of accuracy. (L. Davidsson 2003)

In general, it is difficult to claim which of these two commonly used turbulence modeling techniques to be absolutely more superior. As a matter of fact, the superiority of these models is strongly dependent on not only the nature of the problem and simulation but also the expertise and experience of the CFD user. For example, (Lokhande et al) have suggested the use of the k–e turbulence model for aerodynamic characteristics and LES turbulence model for the analysis of aero acoustic characteristics.

Based on their suggestion, present study combines the RNG k–e turbulence model, a variation of the standard k–e turbulence model, and the LES turbulence model to compute the aerodynamic and aero-acoustic characteristics of a car and its grille. The computational process consists of two steps. In the first step, the overall aerodynamics and front grille of the passenger car and it is estimated using the RNG k–e turbulence model. This computational result is then used as the initial condition for the second step. In the second step, the LES turbulence model is then used to predict the fluctuation of pressure on the surface of the car body and the grille which is attributed to the generation of noise.

2.2.1. K-e Turbulence model

To account for the turbulence effect on the flow field, Reynolds time averaging technique was employed on the Navier-Stokes equation to yield the Reynolds Averaged Navier-Stokes (RANS) equation which can be mathematically expressed as

$$\frac{\partial u_i}{\partial x} + u_j \frac{\partial u_i}{\partial x_i} = -\frac{1}{\rho}\frac{\partial y}{\partial x_i} + \frac{\partial}{\partial x}\left(v\frac{\partial u_i}{\partial u_j} - \tau_{ij}\right); i = 1,2,3; j = 1,2,3 \qquad (10)$$

where the bar on top of the variables implies that the variables are the time-averaged quantities. In Eq. (11),m is the effective viscosity while i, j is the shear-stress tensor. Eq. (10) is impossible to resolve due to the appearance of the Reynolds stress. To bring closure to the above equation, the Reynolds stress term is modeled through the means of k–e turbulence modeling technique.

2.2.2. Boundary Layers And Wall Function

When a fluid flows along a body, a boundary layer is created near the surface and the velocity of the flow is zero, the velocity grows and reaches the freestreem velocity. The thickness of the boundary layer is defined as the distance from the body to where the velocity reaches 99% of the freestream velocity. The boundary layer starts as laminar when the body is exposed to the fluid, as the fluid develops along the body it becomes more turbulent. A laminar boundary is to prefer since the skin friction is lower than for a turbulent layer in certain applications. The near wall flows is usually divided into three regions, the viscous sublayer, buffer layer and the fully turbulent log-low region.

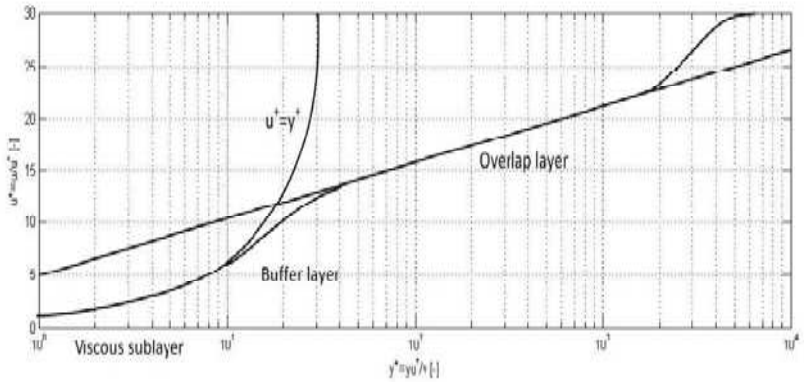

Figure 2.1 : Velocity profile in the near wall region for a turbulence boundary layer

Source: Johan levin et al (2011)

$$y^+ = \frac{yu*}{\mathrm{v}} \tag{11}$$

$$u* = 0.05U \tag{12}$$

Where u* is the friction velocity, v is the kinematic viscosity and y is the height of the first cell. In the normal case, the thickness first cell must have a $y^+ = 1$. In Fluent there are two kinds of wall functions, standard wall functions and non-equilibrium wall functions. Wall function assumes that the flow near the wall behaves fully turbulent and use the algorithm to resolve the gradients in the boundary layer. In no-equilibrium

wall functions the sensitivity for the pressure-gradient are higher then for the standard wall functions.

2.3. Aerodynamic

Aerodynamics is the study of a solid body moving through the atmosphere and the interaction which takes place between the body surfaces and the surrounding air with varying relative speeds and wind directions (Heinz, 2002). Aerodynamics drag is usually neglected at low vehicle speed but the magnitude of air resistance becomes important with the rising speed. This can be seen in Figure 2.2 below which compares the aerodynamics drag forces of a weak streamlined and highly streamlined for vehicle with difference velocity. A vehicle with high drag resistance tends to deceleration the vehicle. When increase the speed, the fuel consumption efficiency is getting worst.

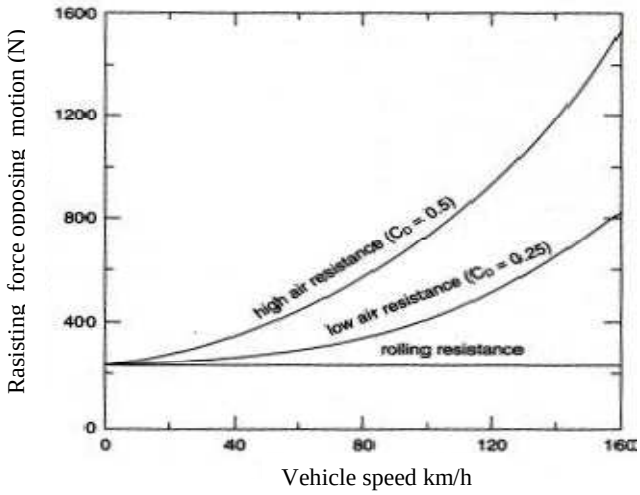

Figure 2.2: Comparison of low and high aerodynamic drag forces with rolling Resistance

Source: Heinz et al, (2002)

Aspects of vehicle aerodynamics passenger compartment all depends on the flow field around and through the vehicle (Cengel, Cimbala, 2006). The external flow around a vehicle is shown in Figure 2.3. In still air, the undisturbed velocity V is the road speed of the car. Provided no flow separation takes place, the viscous effects in the

fluid are restricted to a thin layer of a few millimeters thickness, called the boundary layer, beyond this layer the flow can be regarded as in viscid, and its pressure is imposed on the boundary layer. Source: (Koike et al 2004)

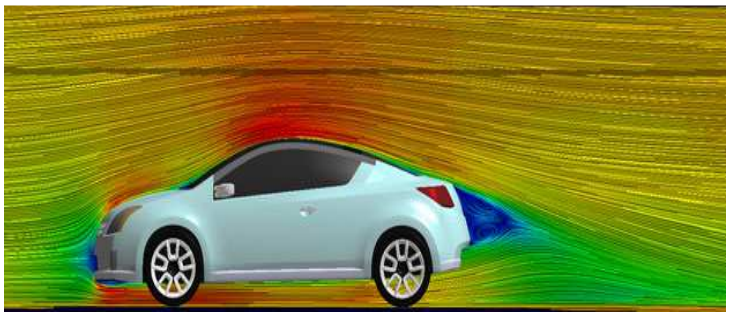

Figure 2.3: Flow around a passenger car (external flow).

Source: Koike et al.(2004)

2.3.1. Aerodynamic Force

The aerodynamics of the vehicle also plays an important role in the design of the cooling system. The opening sizes for the grille and lower valance often limit the amount of "ram" air available to the heat exchangers cooling drag is the unavoidable penalty of integrating a 'cooling module' into a vehicle. It is defined as the drag difference by opening and closing the front-end opening.

From (Williams 2008), the following two factors can be considered as causes for generation of cooling drag:

1. Internal drag is the momentum loss of the grille airflow (cooling + leakage) through the heat exchangers and under hood compartment.
2. External drag is the interference of the grille airflow on the external pressure distribution. It is usually on the external pressure distribution and favorable. Realistically though, the most effective way reduce cooling drag is to focus on the internal component.

2.3.1.1.Drag Force and Drag Coefficient

Drag Force is the force a flowing fluid exerts on a body in the flow direction. Drag force consists of skin drag and pressure drag. Equation (9) (Cengel, Cimbala, 2006) shows relation between friction drag and pressure drag. Frontal pressure is caused by the air attempting to flow around the front of the car. As millions of air molecules approach the front part of the car, they begin to compress, and in doing so raise the air pressure in front of the car.

$$\text{Drag force, } F_D = F_{D,fric} + F_{D,press}, \tag{13}$$

$$\text{Drag coefficient, } c_d = \frac{F_d}{\frac{1}{2}\rho U^2 A} \tag{14}$$

2.3.1.2.Lift Force and Lift Coefficient

The airflow around vehicle usually cause lift force. The components of the pressure and wall shear stress in the direction normal to the flow (perpendicular) tend to move the body in that direction, and their sum is called lift. To some degree, body panel shape and to a larger extent, air that passes through the opening of the grille and under the front end sheet metal. At speed, this massive air stream builds up tremendous pressure under the hood where it is forced to exit rearward, below the chassis, resulting in body lift (Cengel, Cimbala, 2006).

$$\text{Lift force, } F_L = \frac{\rho C_L A V^2}{2} \tag{15}$$

$$\text{Lift coefficient, } C_L = \frac{F_L}{\frac{1}{2}\rho U^2 A} \tag{16}$$

2.3.1.3.Pressure Coefficient

A useful parameter to compare incompressible flows is the pressure coefficient (Cp), see Eq. (17). The pressure coefficient (Cp) describes how the pressure on a

surface deviate from the freestream pressure. Every single point in the flow field or on the surface has an unique Cp. To find the stagnation pressure on a surface Cp should be equal to one. If Cp instead is equal to zero this indicates a low pressure region where the risk for separation is high. In Eq. (17) the pressure coefficient is expressed in terms of pressure.

$$C_P = \frac{p-p_\infty}{\frac{1}{2}\rho U^2} = \frac{p-p_\infty}{dynamic\ pressure} \tag{17}$$

2.4. Front Grill

Recent trends of high engine power are leading to increased airflow requirements for engine cooling and climate control. The greater airflow need drives larger frontal opening with less restrictive grille texture. The pressure drop should be kept as low as possible. Oversized frontal opening will increase vehicle drag and reduce fuel economy. The shape of the vehicle front-end and this charge flow field under the hood and body also impact the area requirement.

2.4.1. Airflow Ducting Between Air Intake And Radiator

The overview on the drag and lift increase caused by current cooling system indicated already that ducting between air intakes and radiator bring about considerable advantages. Volker Renn made the comparison of a typical air intakes and radiator arrangement with and without devices confirms this fact.

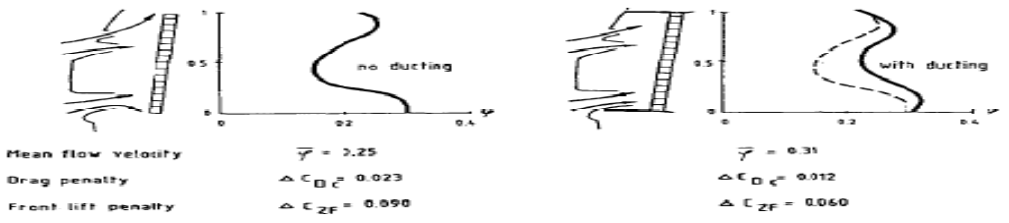

Figure 2.4 : Influence of ducting between air intake and radiator

Source : Volker Renn (1996)

The cooling drag penalty is reduced by close 50% and the front lift is considerably smaller. Ate the same time the mean flow velocity through the radiator is increased by 20% and the velocity distributed is equalized. It can be concluded that cooling performance is greatly improved. (Volker Renn et al 1996).

2.4.2. Location And Size Of Front End Openings

Volker Renn shows the relation of cooling drag and mean radiator flow velocity for different air intakes locations and size. The mean flow through the radiator generally increases nearly linearly with opening size for realistic dimensions of air intake area versus radiator core area.

Volker Renn made the conclusion which can be drawn from the diagram is that a certain required mean cooling flow velocity can be ensured with a rather low drag penalty when the openings are positioned near to the stagnation point.

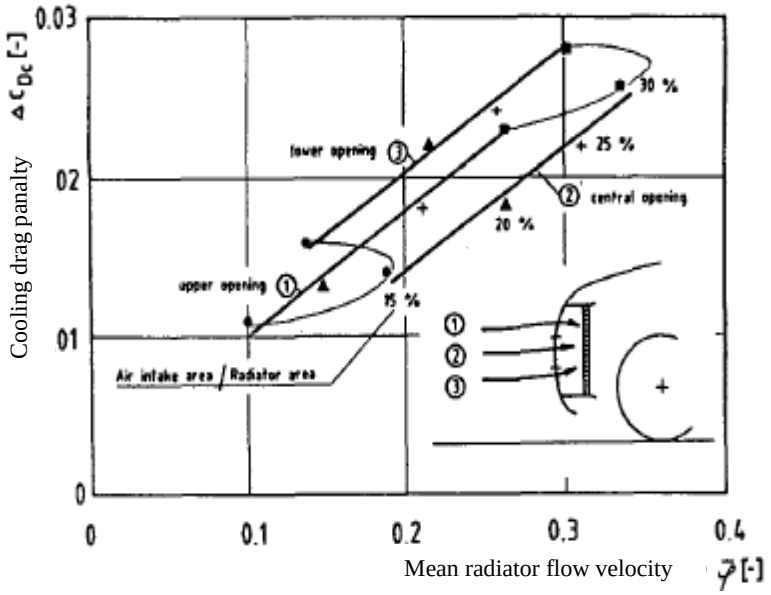

Figure 2.5 : Influence of air intake location and size on aerodynamic performance (measured on a full scale test vehicle)

Source : Volker Renn (1996)

2.5. Previous Work

Much work exists in the field of automotive engineering and the development of CFD model for flow of underhood vehicle aerodynamic and underhood thermal management. This model allow the user to simulate the effect of the cooling system.

Abdul Ghani et al.(2000) discussed the design of a closed loop climatic wind tunnel..This tunnel presented possibilities for analyzing vehicles under controlled environmental conditions such as varying rainfall type and wind direction. Fluent version 5.3.18 was used as a CFD tool to evaluate and optimize the key components of the tunnel. Well established published data and laser sheet visualization (LSV) data provided validation and verification of the CFD result. The result of the investigation was a compact win tunnel with overall dimensions of approximately 3.0 m wide, 9.5 m tall and 9.5 m long.

Spohn and Gillieron (2002) conducted experiments to analyse the flow structures in the wake of a 25° rear slant configuration of Ahmed model in low speed water tunnels. They analysed the flow separations associated in the front and the rear part of the model, along with the separations on the body and also the generation of vortical structures in the near wake region of the model. From their experiments, the flow separations on the roof of front part revealed the existence of separation lines, ending laterally into two foci on either side as the origin for the two counter rotating vortices as shown in figure 2.6 Spohn and Gillieron (2002) .

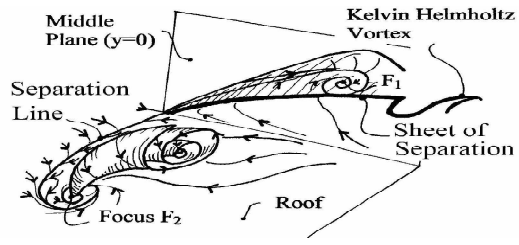

Figure 2.6: Flow separations at front and rear part of Ahmed model geometry

Source: Spohn and Gillieron (2002).